Journal of Power Sources, 43–44 (1993) 39–46

Some aspects on the preparation, structure and physical and electrochemical properties of Li_xC_6

R. Yazami*

Laboratoire d'Ionique et d'Electrochimie du Solide, Institut National Polytechnique de Grenoble, B.P. 75, 38402 St-Martin-d'Hères (France)

D. Guérard

Laboratoire de Chimie du Solide Minéral, Université de Nancy–1, B.P. 239, 54506 Vandœuvre-lès-Nancy Cedex (France)

Abstract

Lithium can be incorporated into a large variety of carbonaceous materials having more or less good crystalline structure organization according to the raw material and to the heat treatment during carbonization or graphitization. Either chemical or electrochemical techniques can be used for the formation of the carbon–lithium intercalation compounds of general formula Li_xC_6. However, the crystallinity of the carbonaceous material and the nature of the electrolyte used for the cathodic reduction play the major role in the stability and the composition of Li_xC_6. This paper intends to review the Li_xC_6 synthesis techniques and to give some results on the electrochemical reversibility and the electrical behaviour of the Li_xC_6/electrolyte interface.

Lithium–carbon compounds: some general aspects

These last few years, very extensive efforts have been oriented towards the development of new reversible negative electrodes for lithium batteries. The main aim of the research work is to overcome the problems of the lithium dendritic growth during the charge operation in batteries using this metal as a negative. Among the proposed replacement materials, carbonaceous ones are now attracting particular interest due to the successive improvements that have been achieved in the faradaic capacity and in the cycle life. This results from the high stability of the carbon/carbon in-plane bonds and the low lattice expansion when 'dry' lithium cations are incorporated between the carbon layers (or graphenes – the relative volumic expansion is $<10\%$ in LiC_6 and around 100% in LiAl [1].

However, some unsolved questions still remain and will surely stimulate the basic research in the future such as the determination of the key parameters that govern the ability of a cabonaceous material to have a good electrode behaviour in terms of low potential, high capacity and long cycle life. One of difficulties arises from the large variety of solid carbon forms which can derive from pitches, mesophase (mixture of optically isotropic and anisotropic phases), cokes (from petroleum or coal), pyrolytic carbon such as that resulting from thermal decomposition of organic polymers, catalytic

*Author to whom correspondence should be addressed.

0378-7753/93/$6.00

carbon, natural or pyrolytic graphites and newly discovered fullerenes. These materials may differ by their chemical composition [2], microtexture (i.e., porosity) and crystalline organization according to the raw material and to heat and/or chemical activation treatments [3]. They also can be shaped in powder, thin films [4] or fibres [5].

Since the electrochemical intercalation and deintercalation of lithium involves charge and mass transfer at the interface between the active carbonaceous electrode and the electrolyte, there should exist a compromise between the crystallinity, which determines the capacity of accomodation of lithium to reach the highest composition LiC_6, and the microtexture which fixes the electrode surface accessible to the electrolyte [6]. By increasing the crystallinity, one generally increases the coherent domains sizes in the (a, b) and c directions (L_a and L_c, respectively) and decreases the microporosity and the surface properties. Natural graphite powder with very high crystallinity has very poor electrochemical lithium intercalation capacity in liquid electrolytes due to the cointercalation of the solvent, such as dimethyl sulfoxide (DMSO) or dimethoxy ethane (DME) [7–9] or to the cathodic decomposition of propylene carbonate (PC) [9–11]. This contrasts with the reported higher capacity and the reversibility of the lithium intercalation from Li^+ organic solutions (mainly PC/DME or PC/ethylene carbonate(EC)) into less well organized pyrolytic carbons [12–14], cokes [15–17] or pitch-based carbon fibres [18]. The effect of heat treatment on the electrode capacity seems to be reciprocal between coke [17] and carbon fibres [18] since it increases in the latter and decreases in the former. On the other hand, the formation of a protective layer at the surface of the carbon electrode during the first lithium intercalation resulting from the partial decomposition of the electrolyte seems to play a major role in its reversible behaviour [15] as it prevents solvent cointercalation and further cathodic decomposition. Similar effects may explain the reversibility of the graphite-based LiC_6 electrode found using solid-state polymer electrolytes in which the lithium cation moves free from any solvating molecules and therefore is intercalated in the 'dry' form [19].

This paper is intended to give a brief review of the chemical and electrochemical intercalation of lithium in different carbonaceous materials with a particular focus on the relation between the structure and microtextural characteristics on the negative electrode behaviour. Some recent results on the LiC_6/liquid electrolyte interface characteristics will also be presented.

Synthesis

Lithium can be intercalated into graphite from gaseous, liquid or solid phases. It leads to different graphite intercalation compounds (GICs) of lithium which differ by their chemical composition (C/Li ratio), colour, stage, etc. The stage number of a GIC corresponds to the number of graphite layers which separate two successive intercalated planes.

Lithium vapour reacts with graphite at 400 °C. This temperature is defined for two reasons: the vapour pressure has to be high enough to allow the intercalation (P_{Li} at 400 °C, $\sim$1 Pa) but the temperature must be lower than 450 °C to prevent formation of lithium carbide Li_2C_2 [20]. The reaction proceeds well with a highly-oriented pyrolytic graphite (HOPG) or single crystals but with lithium powder, the intercalation into graphite occurs only on the top of the powder, the core remains pure graphite [21].

With liquid lithium, one obtains intercalation also mainly with massive samples — due to separation problems — but a temperature of 350 °C is required in order for the core of the sample to be intercalated [22].

TABLE 1

Intercalation of lithium into different carbon varieties

Starting material	Colour	Stage 1	Stage 2	Chemical composition (Li/C)
Petroleum coke HTT 1250 °C	brown yellow	1/3	2/3	6.4
Anthracite	dark blue	from stage 1 to pristine coke		12.3
Glassy carbon V 25	blue	0 pure stage 3	0	30
V 10	blue	1/2	1/2	10.3
Saccharose coke HTT 2500 °C	dark blue	0	1	18
Saccarose coke HTT 1000 °C	black	from stage 1 to pristine coke		
Fiber AG	violet	0	1	22
Fiber AC	blue	0	1	

The compression of mixtures of lithium and graphite powders leads, under pressures of around 2×10^9 Pa, to intercalated phases. It is possible, even at room temperature, to reach the first stage LiC_6 compound; the reaction proceeds in one week. If the compression is followed by annealing at 200 °C at ambient pressure, the complete intercalation is obtained after 24 h [23]. More recently, such intercalation under pressure was shown to lead to compounds with a higher metal concentration: under 6×10^9 Pa, at 280 °C, one obtains either LiC_2 or LiC_4. Those compounds are metastable under ambient temperature and pressure [24].

By these different synthesis methods, one can prepare lithium intercalation compounds which belong to stages 1 to 4. The first stages have defined compositions: LiC_2, LiC_4, LiC_6, whereas for higher stages the composition is variable, for instance, the second stage varies from LiC_{10} to LiC_{20}. First stage compounds have a shiny colour: golden (LiC_6) or slightly silvery (LiC_2 and LiC_4). The second stage phases are purple (LiC_{10} to LiC_{13}) and become steel blue when the lithium content is smaller. The third stages are blue grey and stage 4 presents a colour close to that of pure graphite.

Lithium reacts also with other carbon varieties [25] as shown in Table 1.

In all cases, the product of the reaction — which is performed under the same conditions as for the synthesis of first stage with graphite as host material — is often a mixture of the first and the second stages, even pure second state in some examples.

The main difference concerning the synthesis conditions consists in a much higher tendency of these materials to form lithium carbide. This formation of Li_2C_2 is related to the presence of impurities — as seen in the case of the intercalation into graphite — which are more important in those materials.

Structure

LiC_6 exhibits an hexagonal unit cell which belongs to the space group P6/mmm with one lithium atom in *b* and 6 carbon atoms in *j* (see Fig. 1). The parameters are:

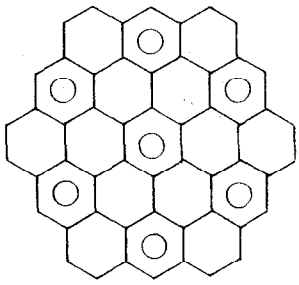

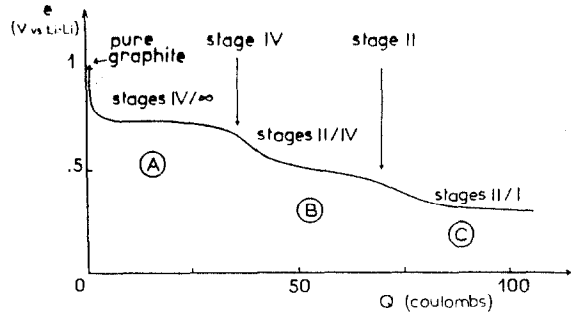

Fig. 1. Schematic diagram of the hexagonal structure in LiC_6.

Fig. 2. Titration curve of Li/(P(OE)$_8$LiClO$_4$/LiC_n at 60 °C; from ref. 19.

$a = 4.305$ Å and $c = 3.706$ Å [25]. The second stage compounds present two defined phases: LiC_{12} whose a parameter is 4.288 Å, close to that of LiC_6 (the difference is connected to the charge transfer) and $c = 7.065$ Å, a value slightly higher than the sum (3.706 + 3.35) Å; this is a general phenomenon in GICs with electron donor) and LiC_{18} also commensurate with respect to the graphite lattice, the a parameter being 7.41 Å. However, it was not possible to detect this lattice since the superstructure reflexions, compared with those of LiC_{12} are very small.

Thermodynamics and kinetics of lithium intercalation

In our previous study [19], we showed that the stage formation during the lithium intercalation into a HOPG using a solid-state poly(ethylene oxide) (PEO)–$LiClO_4$ electrolyte is associated with the observation of successive plateaus in the titration curve as depicted in Fig. 2. The open-circuit voltage (OCV) measurements enable the free energy variation ΔG at 60 °C of each equilibrium to be calculated ($\Delta G = -eF$, e = OCV, F = Faraday constant).

Assuming the ideal chemical compositions of stages 4, 2 and 1 to be formulated as LiC_n (or Li_xC_6 and $x = 6/n$) with $n = 36$, 18 and 6, respectively, we found the following results:

$$36C + Li \rightleftharpoons LiC_{36} \qquad \Delta G_{gr/4} = -16.6 \text{ kcal/Li} \qquad (1)$$

$$LiC_{36} + Li \rightleftharpoons 2LiC_{18} \qquad \Delta G_{4/2} = -11.5 \text{ kcal/Li} \qquad (2)$$

$$1/2LiC_{18} + Li \rightleftharpoons 3/2LiC_6 \qquad \Delta G_{2/1} = -7.7 \text{ kcal/Li} \qquad (3)$$

where $\Delta G_{s_1/s_2}$ designs the variation of the Gibbs energy between stages s_1 and s_2; graphite (gr) corresponds to stage infinite. These values should, however, be taken as indicative only since X-ray diffraction showed that the GICs are in fact composed of a mixture of stages and therefore the n values are average ones.

Intermittent titration techniques introduced by Wen *et al.* [26] enable the intercalation reaction kinetics to be determined. We have calculated the lithium chemical diffusion coefficient into graphite and found $D_{Li} = 5\text{–}7 \times 10^{-8}$ cm^2 s^{-1} at 60 °C. More recent measurements performed at 476 °C in LiCl–KCl eutectic gave D_{Li} values between 10^{-4} and $2\text{–}3 \times 10^{-7}$ cm^2 s^{-1} depending on the composition [27].

Further investigations have been carried out using the same $Li/P(EO)_8$–$LiClO_4/Li_xC_6$ cell and carbon fine powder from natural graphite and led to the formation of the richest ($x=1$) golden phase characteristic of stage-1 GIC [28].

Experimental

Stage-1 LiC_6 was synthesized from HOPG ($4\times4\times0.2$ mm^3 parallelepiped) by immersing it into molten lithium at 200 °C in a stainless-steel reactor maintained under high purity argon atmosphere (<1 volume per million O_2 and H_2O) for two days. The golden colour sample was separated from the unreacted lithium metal by a simple scraping, then it was annealed at 280 °C for several hours and cleaved to obtain a high purity surface. The stage was confirmed by X-ray diffraction analysis and the interlayer spacing deduced from the angular position of the 002 strongest line was found to be $d=3.705$ Å.

Two types of electrochemical test cells were used: (i) a three-electrode cell for the voltammetric studies, the working electrode being the HOPG-based LiC_6, the counter electrode a lithium disc 16 mm in diameter, and a reference electrode consisting of a lithium ring with 16 and 20 mm as internal and external diameter, and (ii) a button-type cell using metallic lithium and LiC_6 as electrodes for the impedence measurements. Potentiostatic measurements were made with low compensating d.c. polarization (2.5 mV = OCV) and 5 mV a.c. voltage amplitude in the frequency range of 65 kHz–0.05 Hz.

The electrolyte consisted of a 1 M solution of $LiBF_4$ in a PC/EC/DME solvent mixture (1:1:2 volumic ratio).

Results and discussion

Cyclic voltammetry

A typical cyclic voltammogram obtained under 10 mV min^{-1} scanning rate and between the electrode potential limits of −100 and 150 mV versus Li^+/Li is showed in Fig. 3. A single anodic peak appears at around 93 mV (curve a) and corresponds to the lithium deintercalation from the LiC_6 electrode following the equation:

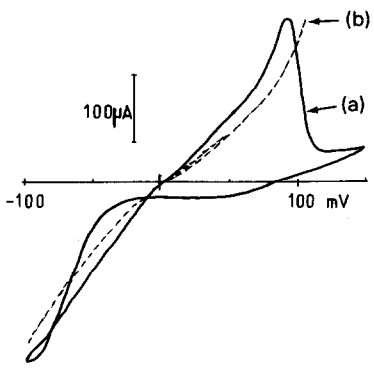

Fig. 3. Cyclic voltammogram at 10 mV min^{-1} scan rate obtained with the Li/electrolyte/LiC_6 three-electrode cell.

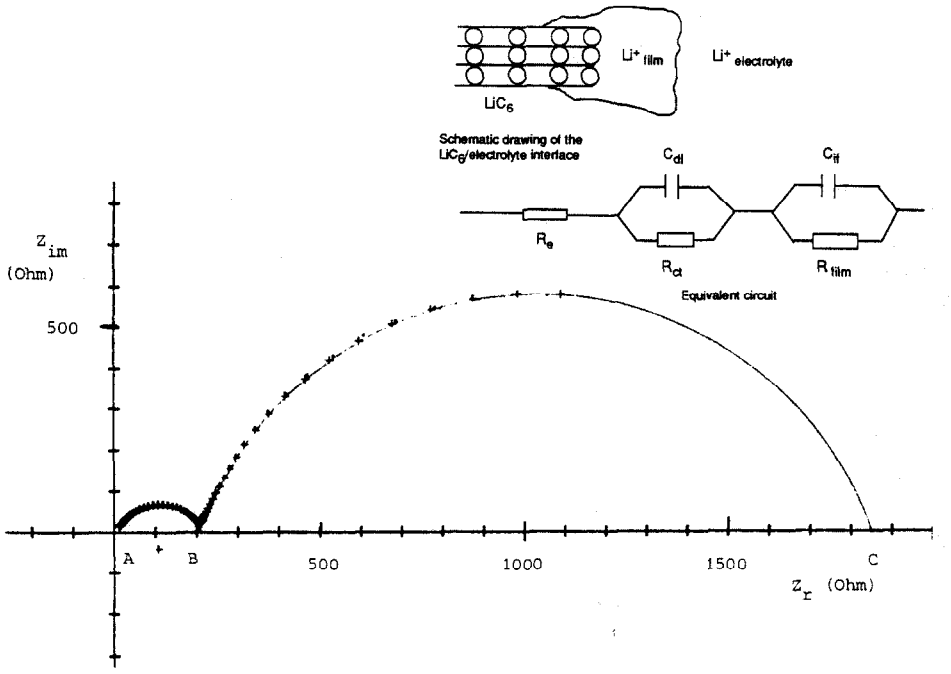

Fig. 4. Impedance spectrum performed between 65 kHz and 0.05 Hz on the Li/electrolyte/LiC_6 cell. Inserts show a schematic representation of the LiC_6/electrolyte interface and the equivalent electrical circuit.

$$LiC_6 \longrightarrow Li_{1-x}C_6 + xLi^+_{solv} + xe^- \quad (4)$$

while at the lithium counter electrode metal cathodic deposition is taking place. To confirm this assumption, a similar cyclovoltammogram was drawn by replacing the LiC_6 electrode by a chip of lithium and is represented by curve b in Fig. 3. It shows no anodic peak. Therefore, the observed anodic behaviour is characteristic of the LiC_6 electrode. When the current was reversed to give cathodic polarization, only a shoulder at about -90 mV was observed which may correspond to the reciprocal of eqn. (4). The asymmetrical shape of the voltammogram indicates that the deintercalation and the reintercalation of lithium from/to LiC_6 do not result from reciprocal mechanisms. When lithium is transferred from the LiC_6 electrode to the liquid electrolyte during the anodic deintercalation, it moves from the 'dry' state to the solvated state (Li^+_{solv}). The solvation free energy contributes to the driving force tending to empty the graphene layers of lithium. The solvation should hinder the lithium transfer from the electrolyte to the LiC_6 electrode which in addition offers only few available sites to accommodate the reduced metal. This may explain the potential delay during the cathodic process.

It is worth noticing that the HOPG-based LiC_6 electrode has a good reversible negative electrode behaviour since it has a very low OCV and overpotential (<10 mV and <90 mV OCV versus the lithium electrode, respectively) and high lithium deintercalation and reintercalation rates.

Impedence spectrometry

The impedence spectrum showed in Fig. 4 can be divided into two 'semi-circles' at high (65 kHz–50 Hz) and low (50–0.05 Hz) frequencies. The equivalent circuit used here to fit the observed results is as shown in the insert, a simple one composed of three resistances (R_e, R_{ct} and R_{film}) and two capacitances (C_{dl} and C_{if}). They are respectively referred to the resistances of the electrolyte, the charge transfer and the protective film and to the capacitances of the double layer and the interface.

This model is consistent with the formation of a protective film at the interface between the solid LiC_6 and the liquid electrolyte (see insert for a schematic representation) as suggested by Fong [15] and Besenhard *et al.* [29]. The lithium cation conducting film should grow as a result of the chemical reduction of the electrolyte solvent by the highly reactive lithium in LiC_6. When the film thickness is sufficient to prevent electron tunneling from the metallic LiC_6, the electrolyte decomposition is stopped. We have observed no low frequency semicircle in a symmetrical cell using two lithium electrodes instead of LiC_6 and the same electrolyte, therefore, its appearance is characteristic of the Li_xC_6 electrode. The film should be somehow inhomogeneous (trapped solvent molecules, incomplete adhesion, etc.) which may explain the observed semicircle characteristic of a diffusion-limited process as for example in porous media [30].

The film has good protective properties since no change in the golden colour of LiC_6 was observed after several months of immersion in the electrolyte in a dry argon atmosphere. This also indicates the good stability of the LiC_6 electrode in appropriate solvents. Further investigations are currently in progress to better characterize the composition, the chemical and the electrical properties of the protective film.

References

1 J. O. Besenhard, J. O. Hess and M. Komenda, *Solid State Ionics, 40/41* (1990) 525.
2 J. Millet, J. E. Millet and A. Vivares, *J. Chem. Phys., 60* (1963) 553.
3 A. Oberlin, *Carbon, 22* (1984) 521–541.
4 J. N. Rouzaud, A. Oberlin and C. Berry-Bassez, *Thin Solid Films, 105* (1983) 75; J. Goma and M. Oberlin, *Thin Solid Films, 65* (1980) 221.
5 M. S. Dresselhaus, G. Dresselhaus, K. Sugihara, I. L. Spain and H. A. Goldberg (eds.), *Graphite Fibers and Filaments,* Springer, Berlin, 1988.
6 R. Kanno, Y. Takeda, T. Ichikawa and O. Yamamoto, *J. Power Sources, 26* (1989) 535.
7 J. O. Besenhard, *Carbon, 14* (1976) 111.
8 J. O. Besenhard, H. Möhwald and J. J. Nickl, *Carbon, 18* (1980) 399.
9 J. O. Besenhard and H. P. Fritz, *Angew. Chem., Int. Ed. Engl., 22* (1983) 950.
10 J. O. Besenhard and H. P. Fritz, *J. Elctroanal. Chem., 53* (1974) 329.
11 M. Arakawa and J. Yamaki, *J. Electroanal. Chem., 219* (1987) 273.
12 R. Kanno, Y. Takeda, T. Ichikawa, K. Nakanishi and O. Yamamoto, *J. Power Sources, 26* (1989) 535.
13 M. Mohri, N. Yanagisawa, Y. Tajima, H. Tanaka, T. Mitate, S. Nakajima, M. Yoshida, Y. Yoshimoto, T. Suzuki and H. Wada, *J. Power Sources, 26* (1989) 545.
14 Y. Nishi, H. Azuma and A. Omaru, *Eur. Patent No. 89 115 940.2.*
15 R. Fong, U. Von Sacken and J. R. Dahn, *J. Electrochem. Soc., 137* (1990) 2009; J. R. Dahn, U. Von Sacken, M. W. Juzkow and H. Al. Janaby, *J. Electrochem. Soc., 138* (1991) 2207.
16 J. R. Dahn, R. Fong and M. J. Spoon, *Phys. Rev. B, 42* (1990) 6424.
17 P. Schoderböck and H. P. Boehm, *Mater. Sci. Forum, 91–93* (1992) 683.
18 M. Sato, T. Iijima, K. Susuki and K. Fujimoto, *Electrochemical Society, Fall Meeting, Seattle, WA, USA, 1990,* p. 64.

19 R. Yazami and P. Touzain, *J. Power Sources, 9* (1983) 365.
20 M. Bagouin, D. Guérard et A. Hérold, *C.R. Acad. Sci., Ser. C., 262* (1966) 557.
21 D. Guérard, *Thesis,* University of Nancy, 1974.
22 D. Billaud and A. Hérold, *Carbon, 13* (1979) 183.
23 D. Guérard et A. Hérold, *C. R. Acad. Sci. Ser. C., 275* (1972) 571.
24 V. V. Avdeev, V. A. Nalimova and K. N. Semenenko, *High Pressure Res., 6* (1990) 11.
25 D. Guérard and A. Hérold, *Carbon, 13* (1975) 337.
26 C. J. Wen, B. A. Boukamp, R. A. Huggins and W. Weppner, *J. Electrochem. Soc., 126* (1979) 2258.
27 R. R. Agarwal, *J. Power Sources, 25* (1989) 151.
28 A. Damasse, Ph. Touzain and R. Yazami, Personal communication.
29 J. O. Besenhard, P. Castella and M. W. Wagner, *Mater. Sci. Forum, 91–93* (1992) 683.
30 J. Thevenin and R. H. Muller, *J. Electrochem. Soc., 134* (1987) 237.